Reconstruction and Evaluation of the Synthetic Bacterial MEP Pathway in *Saccharomyces cerevisiae*

Siavash Partow[1], Verena Siewers[1], Laurent Daviet[2], Michel Schalk[2], Jens Nielsen[1]*

1 Department of Chemical and Biological Engineering, Chalmers University of Technology, Göteborg, Sweden, **2** Firmenich SA, Corporate R&D Division, Geneva, Switzerland

Abstract

Isoprenoids, which are a large group of natural and chemical compounds with a variety of applications as e.g. fragrances, pharmaceuticals and potential biofuels, are produced via two different metabolic pathways, the mevalonate (MVA) pathway and the 2-C-methyl-D-erythritol 4-phosphate (MEP) pathway. Here, we attempted to replace the endogenous MVA pathway in *Saccharomyces cerevisiae* by a synthetic bacterial MEP pathway integrated into the genome to benefit from its superior properties in terms of energy consumption and productivity at defined growth conditions. It was shown that the growth of a MVA pathway deficient *S. cerevisiae* strain could not be restored by the heterologous MEP pathway even when accompanied by the co-expression of genes *erpA*, *hISCA1* and *CpIscA* involved in the Fe-S trafficking routes leading to maturation of IspG and IspH and *E. coli* genes *fldA* and *fpr* encoding flavodoxin and flavodoxin reductase believed to be responsible for electron transfer to IspG and IspH.

Competing Interests: The authors have the following competing interests. Authors L.D. and M.S. declare an interest in FIRMENICH SA as employees of the R&D division. FIRMENICH SA is engaged in the production and commercialization of high-value natural and synthetic ingredients for the flavor and fragrance industry. There are no patents, products in development or marketed products to declare. This does not alter the authors' adherence to all the PLOS ONE policies on sharing data and materials.

* E-mail: nielsenj@chalmers.se

Introduction

In connection with the production of many natural products the transfer of complete biosynthetic pathways from native to heterologous organisms is an attractive approach, as it may allow for use of industrially compatible strains and for further pathway engineering [1,2,3]. Although this approach imposes a number of challenges such as gene codon optimization, correct protein folding and proper enzyme function, there are a several examples where whole biochemical pathways have been transferred successfully such as expressing the mevalonate (MVA) pathway in *Escherichia coli* [4], transferring a complex mammalian hydrocortisone biosynthetic pathway containing 8 genes into yeast [5], and re-construction of the early four steps of the flavonoid biosynthetic pathway in *Saccharomyces cerevisiae* in order to convert phenylpropanoid acids into flavanones [6].

The MVA pathway in yeast and most other eukaryotes and the 2-C-methyl-D-erythritol (MEP) pathway in most bacteria and plant plastids are responsible for production of isoprenoids, which represent an important class of biochemical compounds [7]. The MEP pathway was first reported independently by Rohmer and Argoni [8,9]. This pathway initiates by condensation of one molecule each of pyruvate and D-glyceraldehyde-3-phosphate through a thiamin diphosphate dependent reaction catalyzed by 1-deoxy-D-xylulose 5-phosphate synthase (Dxs) [10], followed by an NADPH dependent reduction process being catalyzed by 1-deoxy-D-xylulose 5-phosphate reductoisomerase (Dxr) [11], generating 2-C-methyl-D-erythritol 4-phosphate (MEP). This intermediate is

converted into the cyclic 2,4-diphosphate of 2-C-methyl-D-erythritol by the sequential action of the enzymes specified by IspD, IspE and IspF [12,13,14]. 2-C-methyl-D-erythritol-2,4-cyclodiphosphate is reduced by a reductase encoded by the *ispG* gene [15,16] followed by the production of IPP and DMAPP by the action of the *ispH* gene product [17,18]. Unlike the MVA pathway, the MEP pathway has not been investigated extensively, in particular in heterologous hosts. *S. cerevisiae* is widely used as a platform for heterologous expression of biochemical pathways [5,19,20], due to its well-characterized physiology and the availability of molecular biology tools. Maury and co-workers reported the reconstruction of the bacterial MEP pathway in *S. cerevisiae* by expression of seven enzymatic steps of the pathway from self-replicating, high-copy yeast plasmids [21]. By inhibiting the endogenous MVA pathway through addition of lovastatin, it was shown that the MEP pathway was active and could ensure production of ergosterol, which is essential for yeast. However, transferring entire biochemical pathways using episomal plasmids is not recommended for industrial applications due to poor genetic stability. In addition, maintenance of plasmids requires selective pressure provided by selective media which increase the costs. In contrast, gene integration offers a stable manipulation without requirement of selective pressure provided through the media.

In this work, we show by using genome-scale modeling that transferring the entire bacterial MEP pathway into *S. cerevisiae* gives a higher theoretical maximum yield of the isoprenoid precursor compared with biosynthesis via the endogenous MVA pathway. In order to activate this pathway in yeast eight enzymatic steps of the

bacterial MEP pathway were integrated into the chromosome of *S. cerevisiae*. Following expression of the heterologous MEP pathway, we found that the IspG and the IspH enzymes are potential bottlenecks of the MEP pathway in *S. cerevisiae* and activating them requires the successful transfer of Fe-S clusters to these two enzymes and a suitable electron transfer system. Therefore, both possible Fe-S trafficking routes responsible for maturation of IspG and IspH and a bacterial electron transfer system were re-constructed in the yeast cytosol by co-expression of the bacterial gene *erpA* with *iscA* from either human or *Arabidopsis thaliana* and flavodoxin and flavodoxin reductase, respectively. These genetic modifications were accompanied with over-expression of *IspG* and *IspH* from *A. thaliana*. However, introducing the above mentioned manipulations did not result in a functional MEP pathway in *S. cerevisiae*.

Based on this study we suggest that specific physical interaction or compartmentalization is required for *in vivo* biogenesis and transfer of essential prosthetic groups, in this case transfer of iron-sulfur clusters, into apoIspG and apoIspH and consequently activation of the bacterial MEP pathway.

Results

In silico Evaluation of MVA and MEP Pathway in *S. cerevisiae*

Seven genes responsible for the enzymatic steps of the bacterial MEP pathway (Figure 1) were introduced into the yeast genome scale metabolic model iIN800 [22]. The efficiency of the MEP pathway was evaluated and compared with the endogenous MVA pathway using the model. The model was optimized for maximum production of farnesyl pyrophosphate (FPP), which is a branch point intermediate in ergosterol biosynthesis, for two different conditions, using the endogenous MVA pathway and using the heterologous MEP pathway, respectively. The result showed that by consuming 1 mol of glucose 0.21 and 0.24 mol farnesyl pyrophosphate could be produced through the MVA and MEP pathway, respectively. According to this analysis the FPP production through the MEP pathway results in a favorable theoretical yield.

The stoichiometry calculation of NAD(P)H and ATP consumption for both pathways showed that for producing one molecule of farnesyl pyrophosphate from glucose via the MVA pathway six molecules of NADPH and nine molecules of ATP are required, while production via the MEP pathway consumes nine molecules of NAD(P)H and six molecules of ATP. Provision of sufficient cytosolic NADPH is therefore a critical factor for both pathways. In contrast to the MEP pathway, which consumes only 3 molecules of glucose, the MVA pathway consumes 4.5 molecules of glucose for the biosynthesis of one molecule farnesyl pyrophosphate (these values are excluding use of glucose for production of ATP and redox co-factors).

Combining the results derived from the yeast genome scale metabolic model and the stoichiometry calculation, it became evident that the MEP pathway is a more efficient route than the endogenous MVA pathway for isoprenoid production in terms of energy consumption and productivity. Therefore we decided to investigate this pathway in *S. cerevisiae*, which has been widely used as a platform for heterologous expression of isoprenoids [19,20].

Genomic Integration of MEP Pathway Genes

Since the efficiency of *in vivo* homologous recombination in *S. cerevisiae* is high, a bipartite integration strategy was applied [23]. Eight codon optimized MEP pathway genes including *dxs*, *dxr*, *ispD*, *ispE*, *ispF*, *ispG*, *ispH* and *idi* were organized in four different synthetic fragments (Figure 2A). Each fragment contained two genes located on each side of the bidirectional promoter P_{TEF1}-P_{PGK1}, which had shown high constitutive activity in glucose containing media before [24], and in front of either the *ADH1* or the *CYC1* terminator. Furthermore, each fragment harbored a part (ca. 2/3) of a gene coding for a selectable marker (*kanMX* or *K.l.URA3*) and flanking regions which corresponded to the desired integration site on the chromosome and which were necessary for integration via homologous recombination. In order to recycle the selectable markers, direct repeat DNA sequences of 143 bp were introduced at both sides of *K.l.URA3*, whereas *loxP* sites flanked the *kanMX* cassette.

Previously, different transcription levels among various chromosomal regions in *S. cerevisiae* have been reported by using *lacZ* as a reporter gene [25]. We have shown that the two integration sites, YPRCΔ15 and YPRCτ3, on chromosome XVI of *S. cerevisiae* provided potentially higher expression levels than other regions tested [25]. Therefore, all genes involved in the bacterial MEP pathway were integrated into these two sites in two steps (Figure 2A). The selectable markers, *kanMX* and *K.l.URA3*, were looped out. Integration and transcription of the MEP genes was confirmed by PCR and RT-PCR, respectively (data not shown). Table 1 lists the strains which were constructed during this work. Strains SCISP06 and SCISP12 were obtained through the integration of MEP pathway genes into the chromosome of CEN.PK 113-13D and CEN.PK 113-1C, respectively.

The functionality of the bacterial MEP pathway was tested by blocking the endogenous MVA pathway which is essential for *S. cerevisiae* because of its supply of ergosterol involved in regulation of membrane fluidity [26]. The MVA pathway was inhibited using lovastatin (mevinolin) [27] which is a therapeutic agent and acts as a competitive inhibitor of an early pathway enzyme, HMG-CoA reductase. Surprisingly, no growth was observed in both wild type (CEN.PK 113-13D) and SCISP06 (yeast strain with integrated MEP pathway) in presence of 2 g L^{-1} lovastatin (Figure 3), respectively, which showed that the MEP pathway could not complement the MVA pathway, and which is in contrast to the previous report [21].

Re-construction the Possible Bacterial Fe/S Trafficking Routes and the Bacterial Electron Transfer System

The detection of intermediates 3 and 5 (Figure 1) in the MEP-pathway carrying yeast strains indicated proper activity of the Dxs, Dxr and the IspD enzymes (data not shown). In addition, no-activity was observed for the last two enzymes of the MEP pathway, IspG and IspH, when expressed in yeast in a previous study [28]. IspG and IspH are known to be iron-sulfur cluster proteins [15,16,17,29,30,31] and it has been reported that this cluster is directly involved in IspH activity [32]. The essential role of ErpA, which is an A-type iron-sulfur cluster protein, in the maturation process of IspG, and probably IspH, in *E. coli* has been investigated [33]. Furthermore, Puan and co-workers [34] identified *fldA* as an essential gene for isoprenoid biosynthesis in *E. coli*, as it provides reducing equivalents for the Fe/S clusters of IspG and IspH. *FldA* encodes flavodoxin I, which together with *fpr* encoded flavodoxin reductase composes an *E. coli* electron transfer system [35]. As an attempt to solve the problem of the non-functionality of the MEP pathway in *S. cerevisiae*, the impact of the co-expression of genes involved in transferring Fe-S clusters to IspG/IspH apoproteins and of the described *E. coli* electron transfer system was investigated. The coding region of genes *erpA*, *fpr* and *fldA* from *E. coli* were cloned on a single plasmid, pISP08, (Figure 2B) that was transformed into SCISP06 generating SCISP16 (Table1). The empty plasmid pSP-GM1 was trans-
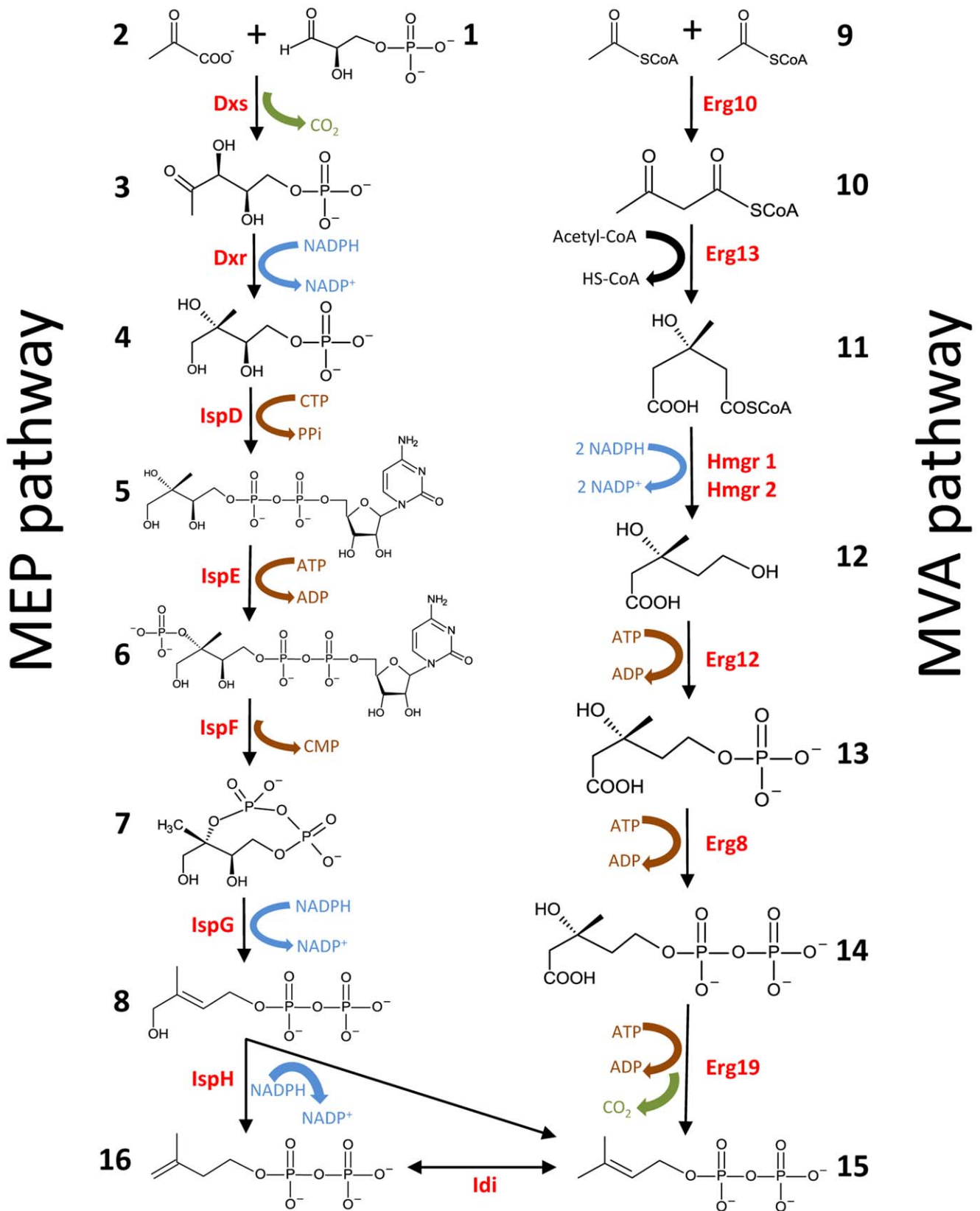
Figure 1. The MEP pathway (left). Enzymes: **Dxs,** 1-deoxy-D-xylulose-5-phosphate synthase; **Dxr,** 1-deoxy-D-xylulose 5-phosphate reductoisomerase; **IspD,** 4-diphosphocytidyl-2-C-methyl-D-erythritol synthase; **IspE,** 4-diphosphocytidyl-2-C-methylerythritol kinase; **IspF,** 2-C-methyl-D-erythritol 2,4-cyclodiphosphate synthase; **IspG,** 4-hydroxy-3-methylbut-2-en-1-yl diphosphate synthase; **IspH,** 1-hydroxy-2-methyl-butenyl 4-diphosphate reductase; Metabolites: **1,** D-glyceraldehyde 3-phosphate; **2,** pyruvate; **3,** 1-deoxy-D-xylulose 5-phosphate; **4,** 2-C-methyl-D-erythritol

4-phosphate; **5,** 4-diphosphocytidyl-2-C-methyl-D-erythritol; **6,** 2-phospho-4-diphosphocytidyl-2-C-methyl-D-erythritol; **7,** 2-C-methyl-D-erythritol 2,4-cyclodiphosphate; **8,** 1-hydroxy-2-methyl-2-(E)-butenyl 4-diphosphate. The MVA pathway (right). Enzymes: **Erg10,** acetoacetyl-CoA thiolase; **Erg13,** 3-hydroxy-3-methylglutaryl-CoA synthase; **Hmg1/2,** 3-hydroxy-3-methylglutaryl-CoA reductase; **Erg12,** mevalonate kinase; **Erg8,** phosphomevalonate kinase; **Erg19,** mevalonate diphosphate decarboxylase; **Idi,** isopentenyl diphosphate isomerase; Metabolites: **9,** acetyl-CoA; **10,** acetoacetyl-CoA; **11,** 3-hydroxy-3-methylglutaryl-CoA; **12,** mevalonate; **13,** phosphomevalonate; **14,** diphosphomevalonate; **15,** isopentenyl diphosphate; **16,** dimethyl allyl diphosphate.

formed into CEN.PK113-13D and SCISP06 resulting in SCISP28 and SCISP29, respectively (Table 1).

To rule out any possible additional effect on cell growth using lovastatin for inhibition of the MVA pathway the functionality of the bacterial MEP pathway was investigated by deletion of *ERG13*, an essential gene in the MVA pathway. *ERG13* encodes HMG-CoA synthase [7], and its disruption results in a strain that requires exogenous mevalonate supplementation for viability [36]. The

coding region of *ERG13* in strains SCISP16, SCISP28 and SCISP29 was replaced by a *kanMX* integration cassette, which was confirmed by PCR (Figure 4A). As it is illustrated in Figure 4B, the *ERG13* deleted strains could not grow in media lacking mevalonate under aerobic conditions.

Since bacterial IspG and IspH have not shown any activity in yeast [28], we asked whether a eukaryotic version of both IspG and IspH would be active in yeast; the codon optimized plant
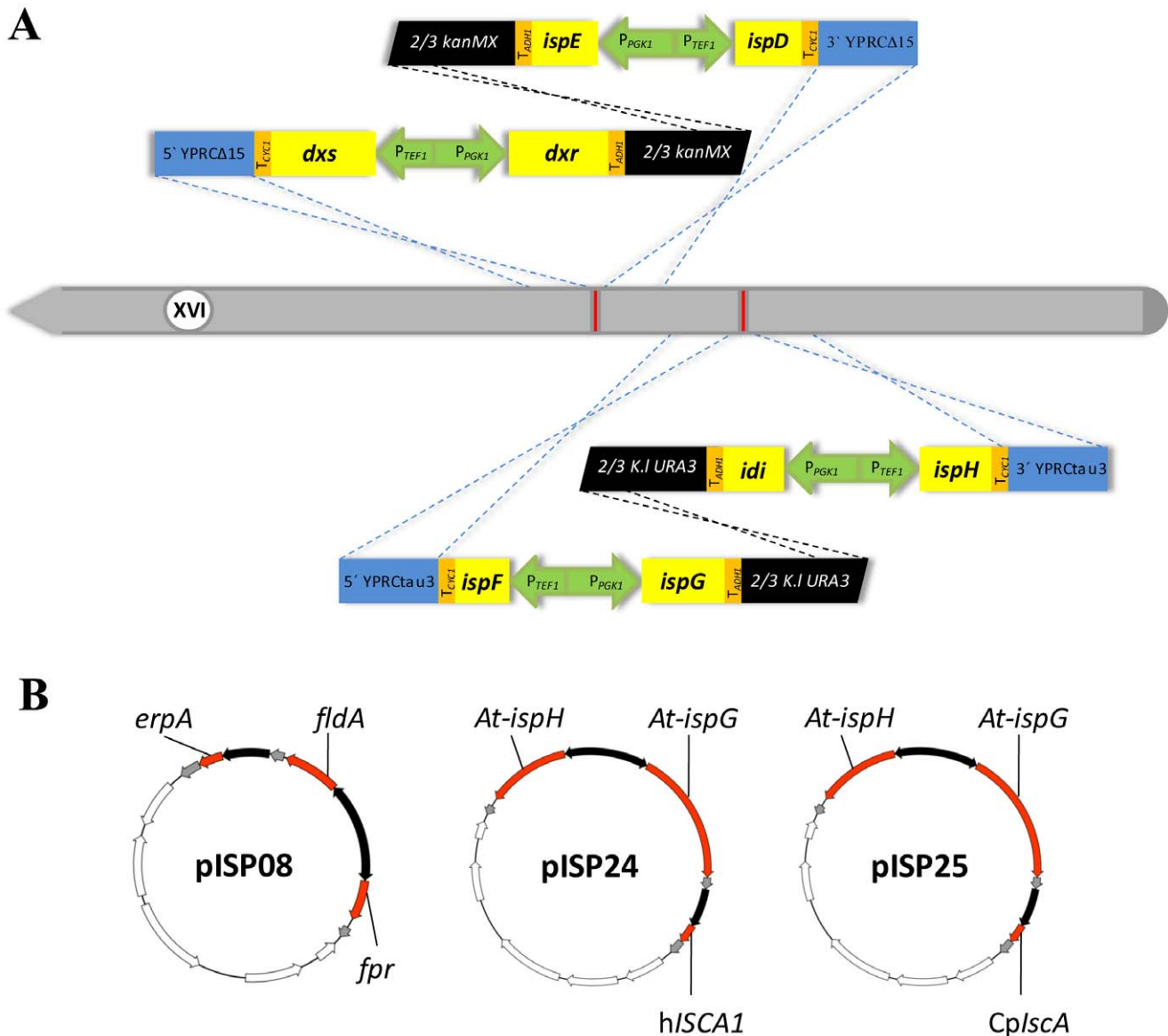
Figure 2. Schematic representation of genetic engineering strategies for A) genomic integration of the bacterial MEP pathway genes into the yeast genome (chromosome XVI), and B) plasmid-based reconstruction of possible Fe/S trafficking routes involved in maturation of bacterial IspG/IspH, bacterial electron transfer systems and plant-derived *ispG/ispH* in *S. cerevisiae.* For details see text.

Table 1. List of strains and plasmids used in this study.

Strain	Genotype	Plasmid	Reference
CEN.PK 113-13D	*MATα MAL2-8c SUC2 ura3-52*	None	P. Kötter[1]
SCISP06	*MATα MAL2-8c SUC2 ura3-52 dxs dxr ispD ispE ispF ispG ispH idi*	None	this work
SCISP16	*MATα MAL2-8c SUC erg13::loxP-KanMX-loxP dxs dxr ispD ispE ispF ispG ispH idi*	pISP08	this work
SCISP28	*MATα MAL2-8c SUC2 erg13::loxP-KanMX-loxP,*	pSP-GM1	this work
SCISP29	*MATα MAL2-8c SUC2 erg13::loxP-KanMX-loxP dxs dxr ispD ispE ispF ispG ispH idi*	pSP-GM1	this work
CEN.PK 113-1C	*MATa MAL2-8c SUC2 trp1-289 ura3-52 his3Δ1*	None	P. Kötter[1]
SCISP12	*MATa MAL2-8c SUC2 trp1-289 ura3-52 his3Δ1 dxs dxr ispD ispE ispF ispG ispH idi*	None	this work
SCISP13	*MATa MAL2-8c SUC2 trp1-289 his3Δ1 dxs dxr ispD ispE ispF ispG ispH idi*	pISP08[2]	this work
SCISP30	*MATa MAL2-8c SUC2 trp1-289 erg13::loxP-KanMX-loxP*	pSP-GM1, pSP-GM3	this work
SCISP31	*MATa MAL2-8c SUC2 trp1-289 erg13::loxP-KanMX-loxP dxs dxr ispD ispE ispF ispG ispH idi*	pISP08, pISP24[3]	this work
SCISP32	*MATa MAL2-8c SUC2 trp1-289 erg13::loxP-KanMX-loxPdxs dxr ispD ispE ispF ispG ispH idi*	pISP08, pISP25[4]	this work

[1]University of Frankfurt, Germany.
[2]pISP08 contains *erpA, fpr* and *fldA*.
[3]pISP24 contains *hISCA1, At-IspG* and *At-IspH*.
[4]pISP25 contains *CpIscA, At-IspG* and *At-IspH*.
doi:10.1371/journal.pone.0052498.t001

genes of IspG and IspH from *A. thaliana* were chemically synthesized. In addition, an Fe-S trafficking model has previously been proposed that describes the transfer of Fe-S clusters to IspG and IspH in *E. coli* (Figure 5) [37]. The authors suggested that depending on the environmental conditions e.g. aerobic, anaerobic or stress, the Fe-S cluster is transferred from IscU or SufU scaffolds to apoIspG and apoIspH through the combination of A-type carriers including ErpA, IscA and SufA [37]. Assuming that

this model can be transferred from *E. coli* to yeast the expression of *iscA* may fill the gap in this proposed model [37]. Therefore, one copy of each *IspG* and *IspH* from *A. thaliana* was cloned into expression plasmids with *iscA* from either human or *A. thaliana* resulting in pISP24 and pISP25, respectively (Figure 2B). Previously, localization and activity of human ISCA1 (hISCA1) was shown in mitochondria as well as in the cytosol of HeLa cells [38]. The authors have also demonstrated interaction of the small
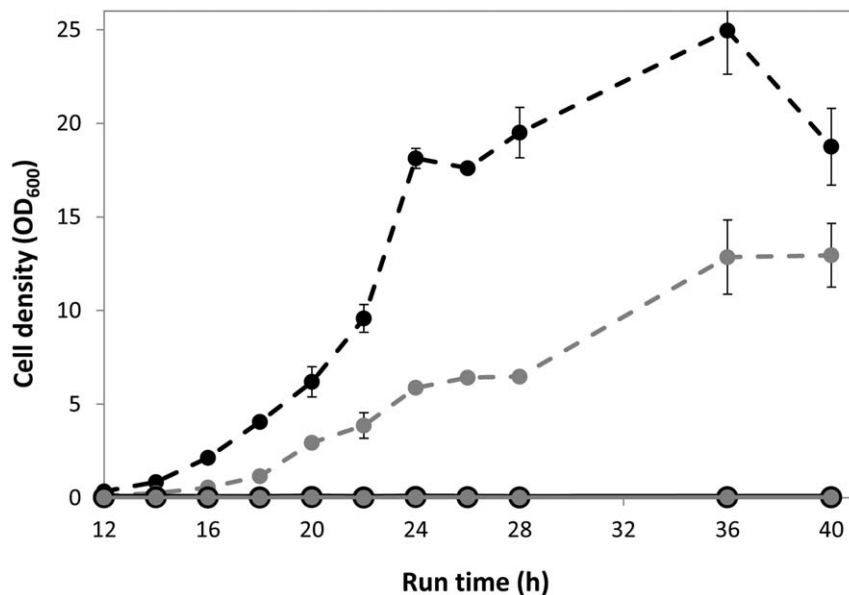
Figure 3. Growth of *S. cerevisiae* strains CEN.PK 113-13D (black circles) and SCISP06 (gray circles) in SD minimal medium. Dashed lines represent the growth in 0 g L^{-1} of lovastatin; solid lines represent the growth in presence of 2 g L^{-1} of lovastatin. Error bars show the standard deviation from three cultivations.
doi:10.1371/journal.pone.0052498.g003
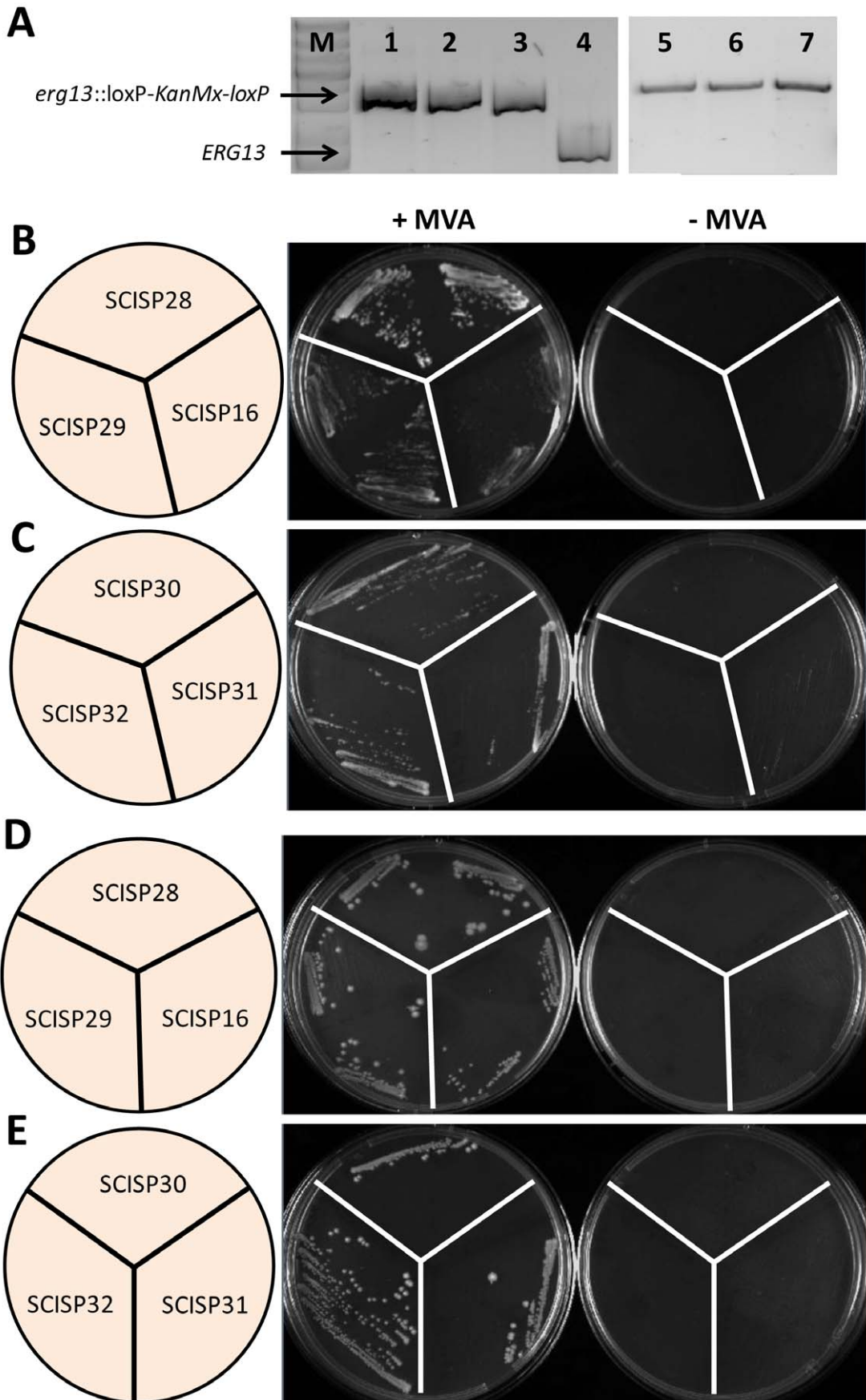
Figure 4. Schematic representation of evaluation the functionality of the bacterial MEP pathway in *S. cerevisiae* in different conditions. A) Gel electrophoresis of PCR products to confirm deletion of *ERG13* (1: SCISP28, 2: SCISP29, 3: SCISP16, 4: CEN.PK 113-13D (wild type), 5: SCISP30, 6: SCISP31, 7: SCISP32, M: 1 kb Plus DNA ladder (Fermentas, Maryland, USA); **B)** Aerobic cultivation of MEP pathway strains co-expressing *erpA, fpr* and *fldA*; **C)** Aerobic cultivation of MEP pathway strains co-expressing *erpA, fpr, fldA, At-IspG, At-IspH* with either *CpIscA* or *hISCA1*; **D)** Anaerobic cultivation of MEP pathway strains co-expressing *erpA, fpr* and *fldA*; E) Anaerobic cultivation of MEP pathway strains co-expressing *erpA, fpr, fldA, At-IspG, At-IspH* with either *CpIscA* or *hISCA1*. All strains carried an *ERG13* deletion and were plated on medium with or without 10 mg L^{-1} mevalonate (MVA).

domain of IOP1 (**I**ron-**o**nly hydrogenase-like **p**rotein **I**) with human ISCA1 using yeast two-hybrid systems [38]. CpIscA from *A. thaliana* is involved in Fe-S biogenesis in chloroplasts [39]. The Fe-S cluster in CpIspA indicated stability in presence of oxygen [39]. Strains SCISP31 and SCISP32 were constructed by co-transforming pISP08 with either pISP24 or pISP25 into SCISP12, respectively (Table 1). Like for SCISP16, no growth was observed in the absence of exogenous mevalonate when *ERG13* was disrupted in both SCISP31 and SCISP32 (Figure 4C).

Fe-S clusters are sensitive to superoxide (O_2^-) and other oxidative agents [40,41]. In addition, the Fe-S cluster of IspH is easily destroyed by exposure to molecular oxygen or other oxidative agents [32]. Therefore, to prevent inactivation of the Fe-S clusters in IspG and IspH, all *erg13* strains were also evaluated under anaerobic conditions. Yeast growing in anaerobic condition is ergosterol-dependent as the biosynthetis of ergosterol is disrupted in this condition. Therefore, exogenous ergosterol was added to the SD media at a final concentration of 1 mg L^{-1}. None of the *erg13* strains showed mevalonate-independent growth (Figure 4D and 4E). This means that even in anaerobic conditions, the MEP pathway was not able to complement the MVA pathway.

Discussion

In the current study, the seven enzymatic reactions of the bacterial MEP pathway were evaluated *in silico*, using the yeast genome scale metabolic model, iIN800 [22]. iIN800 consists of 1446 metabolic reactions and 1013 metabolites [22]. In comparison to the first *S. cerevisiae* model by Förster and co-workers [42], iIN800 covers lipid metabolism in great detail. Applying mathematical models has previously been demonstrated to be predictive and beneficial for metabolic engineering approaches e.g. to identify new target genes enhancing the biosynthesis of sesquiterpenes in yeast [43], and to schematically represent the effect of the interaction of protease supplementation and type of sugar on amino acid metabolisms in brewer's yeast [44]. Here, *in silico* analysis of the bacterial MEP pathway expressed in yeast revealed the benefits of this heterologous pathway in terms of energy consumption and yield compared to the endogenous MVA pathway. Our result is in consistence with previous reports about the higher efficiency of the MEP pathway in converting sugars or glycerol into terpenoids compared to the MVA pathway [45,46]. This is the rationale for our attempt to express the bacterial MEP pathway in yeast for production of isoprenoids.

The first step of most yeast metabolic engineering and synthetic biology studies involves re-construction of a complete or partially synthetic pathway. Although several methods have been developed [3,47], *in vitro* DNA synthesis offers a fast, cheap and efficient method for synthesis of large DNA sequences [48,49]. Besides, using synthetic genes with the possibility to manipulate codon bias can provide better control of the expression of heterologous MEP pathway genes in yeast. From the genetic engineering point of view, the codon bias is one of the first barriers in heterologous protein expression [50] and it can prevent the efficient biosynthesis of a recombinant protein because of altering the correlation between the frequency of the codon and the abundance of its

corresponding tRNA, which impairs the translation machinery of the host [51]. The high efficiency and ease to work with *in vivo* homologous recombination in *S. cerevisiae* allows stable manipulation without requiring selective pressure for maintenance. Here we developed a strategy for easy integration of eight heterologous genes. The four DNA constructs containing the eight MEP pathway genes, including expression elements and selection markers were designed *in silico*, synthesized *in vitro* and integrated into the yeast chromosome via homologous recombination. The functionality of this pathway in *S. cerevisiae* was evaluated by the attempt to block the endogenous MVA pathway. Inhibition of the MVA pathway can be achieved using an inhibitor or by deletion of the essential genes of this pathway [26,36,52–55]. Unlike previously reported [21], chemical as well as genetic inhibition of MVA pathway revealed the non-functionality of the MEP pathway. We conclude that the previous result [21] may have derived from incomplete repression of the MVA pathway, even when higher concentrations (2 g L^{-1}) of lovastatin were used, which may result from errors in activation of lovastatin by hydrolysis reducing the actual concentration of the active inhibitor, or the higher-level expression from multi-copy plasmids may have resulted in partial activation of the enzymes resulting in a functional MEP pathway. One could speculate that elevation of the number of mitochondria using galactose as a non-fermentable carbon source in the previous report [21] might have led to the functional MEP pathway. In eukaryotes, these organelles play a central role in maturation of Fe/S proteins in both mitochondria and cytosol. However, the strains presented in our work did not grow in media containing raffinose when the MVA pathway was inhibited using lovastatin (data not shown), and this strongly indicate that our previous claim of an active MEP pathway in yeast was based on lack of proper repression of the MVA pathway as also found in another study [28].

High concentrations of lovastatin could also have caused side effects which mask the operation of the MEP pathway. Thus, the inhibition of Hmg1 and Hmg2 using lovastatin has shown to result in an altered transcriptional response including the up-regulation of genes related to plasma membrane proteins, protein catabolism and ribosome biosynthesis and down-regulation of *MAF1* [56,57] which encodes a repressor of RNA polymerase III [58]. Priviously, Kaminska and co-workers have shown an increase in tRNA levels when Maf1 is diminished [59] and consequently the demand for DMAPP, which is involved in tRNA biosynthesis, was increased [60]. Such requirement may be higher than what is provided by the MEP pathway. Gene deletion in contrast offers absolute inactivation of the MVA pathway. It has been indicated that yeast strains with deficiency in *ERG13, ERG19, ERG8*, or *ERG9* are nonviable at normal growth conditions [26,36,52–55]. Since the MEP pathway contributes to the ergosterol biosynthetic pathway through IPP and DMAPP intermediates, deletion of *ERG13*, *ERG19* or *ERG8* which are located upstream of these intermediates should be more efficient than using lovastatin for blocking the MVA pathway and evaluating the MEP pathway functionality. For our purpose *ERG13* is a good candidate since supplying the medium with exogenous mevalonate can complement its deletion. However, the inability of the *ERG13* deleted strain to grow showed
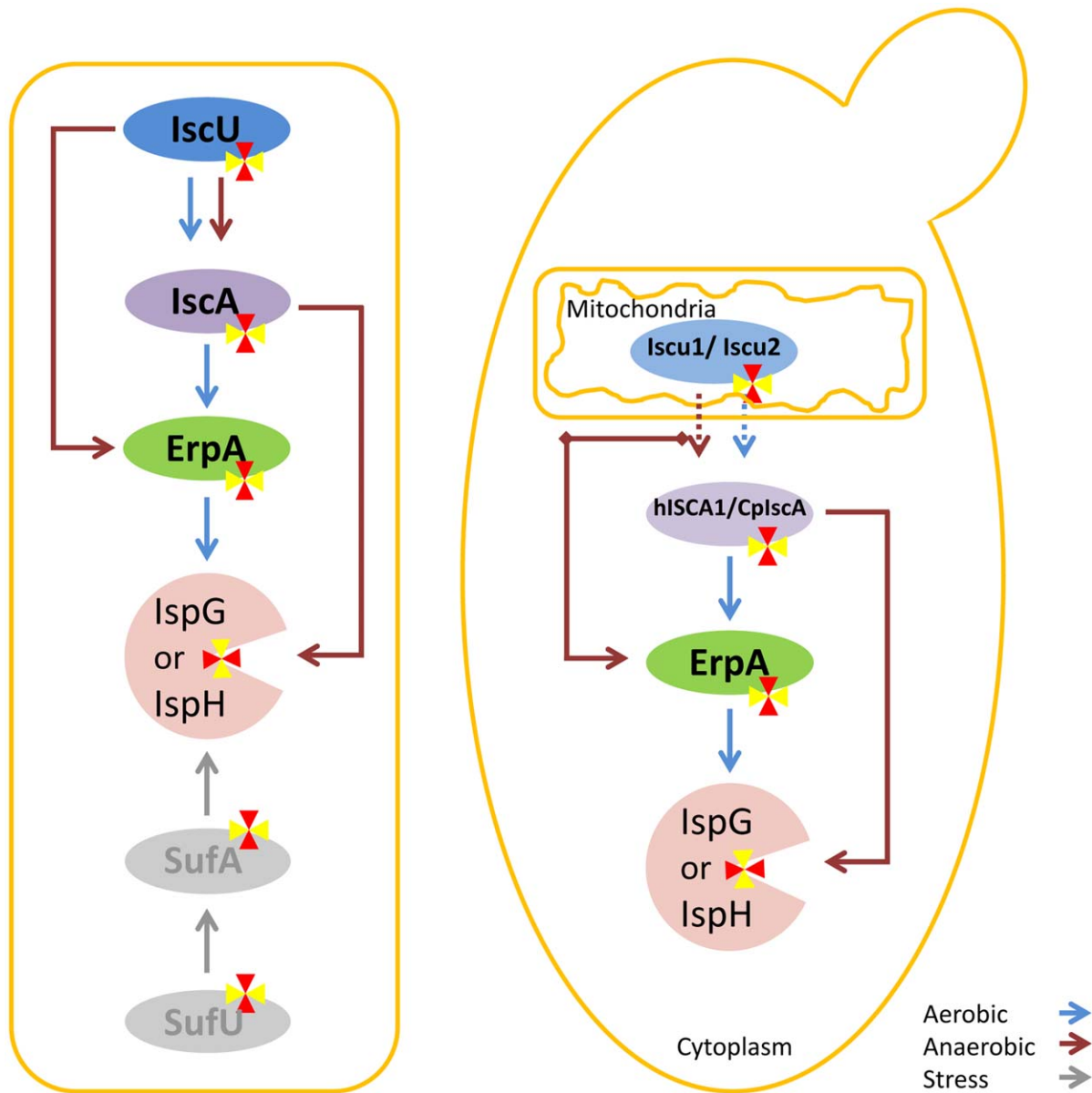
Figure 5. Schematic representation of possible Fe/S trafficking routes involved in maturation of bacterial IspG/IspH in *E. coli* (left) and reconstruction of possible routes preformed in this study in the yeast cytosol (right). Dashed arrows represent unknown mechanisms for transferring the Fe-S clusters from mitochondria to cytosol. For more information see text.
doi:10.1371/journal.pone.0052498.g005

that the MEP pathway could not complement the MVA pathway deficiency.

We hypothesize that a potential reason for the non-functionality of the MEP pathway in *S. cerevisiae* is the lack of the enzyme activity of IspG and/or IspH, which catalyze the last two reactions of the pathway. It has been reported that both enzymes, IspG and IspH, are dependent on NADPH and the flavodoxin/flavodoxin reductase redox system as electron donor for their catalytic activity [17,18,34,61–63]. Gräwert and co-workers [32] have reported that the *in vitro* maximum activity for IspH was obtained with NADPH as co-substrate, together with recombinant flavodoxin and flavodoxin reductase from *E. coli*. Flavodoxin and flavodoxin reductase are FMN and FAD cofactor containing proteins, respectively, and it has been shown that NADPH is the preferred reducing equivalent of flavodoxin reductase compared to

NADH [35]. Overexpression of flavodoxin and flavodoxin reductase might facilitate electron flux from NADPH to IspG and IspH and therefore result in increased the activity of these enzymes. A similar phenomenon was observed in biosynthesis of hydrocortisone in yeast [5]. Overexpression of the essential endogenous reductase Arh1 (adrenodoxin eeductase homolog) using a strong promoter increased the production of hydrocortisone up to 60% [5]. Both Arh1 and human ADX protein (adrenodoxin) are responsible for transferring electrons from NADPH to the related enzyme. The authors suggested that the flux of electrons was elevated as a result of *ARH1* overexpression [5]. Furthermore, both IspG and IspH are known as iron-sulfur cluster proteins which are harboring cubic type of Fe/S clusters, and it has been suggested that these [4Fe–4S] clusters participate in the electron transfer process [15–17,29–31]. Despite the

presence of Fe-S assembly machineries in yeast - the ISC system is present in the mitochondria and the CIA system is used for cytosolic FeS cluster assembly [64–66] - these systems may not be suitable to transfer iron-sulfur clusters to IspG and IspH. Recently, a suitable model has been proposed demonstrating the Fe/S trafficking paths leading to IspG and IspH maturation in *E. coli* [37]. The essential role of ErpA in maturation of the IspG and the IspH enzymes in *E. coli* has been indicated [33]. It was also shown that the Fe-S clusters can directly be transferred from IscU to ErpA in *E. coli* [67]. Based on these findings, the functionality of the bacterial MEP pathway was evaluated in presence of the cytosolic expression of bacterial genes *erpA*, *fpr* and *fldA* in yeast, but we still could not obtain functionality of the enzymes. Previously reported data have shown that the cytosolic localization has failed to generate a functional bacterial or human IscU while expressed in yeast [68]. Even yeast U-type homolog scaffolds (Isu1 and Isu2) playing a crucial role in maturation of both cytosolic and mitochondrial Fe-S proteins need to be expressed in mitochondria to show activity [68].

As illustrated in Figure 5, the Fe-S cluster is transferred to the last two enzymes of the MEP pathway through A-type proteins (IscA, ErpA and SufA) in three different conditions (aerobic, anaerobic and stress) [37]. A-type iron-sulfur carriers (ATCs) have initially emerged in most bacteria before being acquired by eukaryotes and a few archaea by means of horizontal gene transfer [37]. Tan and co-workers have suggested that both IscA and SufA are required for assembly of cubic Fe-S clusters in *E. coli* under aerobic condition [69]. We further constructed possible bacterial paths (aerobic and anaerobic) which are involved in transferring Fe-S clusters to IspG and IspH in the yeast cytosol (Figure 5). Co-transformation of *erpA* with either human *ISCA1* or plant derived *CpIscA* in addition to plant *ispG* and *ispH* and bacterial genes, *fpr* and *fldA* did not result in a functional MEP pathway in both aerobic and anaerobic conditions although human ISCA1 had been shown to have partial cytosolic activity in HeLa cells [38]. *S. cerevisiae* also contains two types of A-type carriers, Isa1 and Isa2, which are localized in the mitochondrial matrix and in the mitochondrial inter-membrane space, respectively [70,71]. The mitochondrial localization is necessary for the functionality of both the Isa1 and the Isa2 protein in yeast [70]. The contribution of these proteins in the maturation process of IspG and IspH in an *E. coli* strain which has a deficiency in *erpA*, *iscA* and *sufA* has been demonstrated [37]. However, it has been demonstrated recently that only Isa1 can be functionally replaced by the bacterial A-type ISC proteins, ErpA, IscA and SufA [72].

In conclusion, we believe that specific physical interaction and compartmentalization would be required for *in vivo* biogenesis and transfer of essential prosthetic groups, here the iron-sulfur clusters for activation of bacterial MEP pathway enzymes in yeast. Therefore, it seems interesting to evaluate IspG and IspH expression in the mitochondria as this may represent a new interesting engineering strategy, which may even be relevant for activation of other bacterial iron-sulfur cluster proteins in yeast.

Materials and Methods

Strain and Plasmid Construction

Sequences of all *E. coli* MEP pathway genes including *dxs* (AAC73523), *dxr* (AAC73284), *ispD* (AAC75789), *ispE* (AAC74292), *ispF* (AAC75788), *ispG* (AAC75568), *ispH* (AAC73140) and *idi* (AAC75927) were used to construct four different integrative fragments (File S1), in which each gene was placed behind a *TEF1* or *PGK1* promoter and in front of a *CYC1* or *ADH1* terminator, respectively (Figure 2). Gene sequences were

codon optimized for expression in *S. cerevisiae* and the four fragments were synthesized by DNA2.0 (Menlo Park, CA, USA). The sequences of the four fragments are presented in File S1.

The synthetic fragments were integrated into *S. cerevisiae* CEN.PK 113-13D (*MATα MAL2-8c SUC2 ura3-52*) and CEN.PK 113-1C (*MATa MAL2-8c SUC2 trp1-289 ura3-52 his3Δ1*) (kindly provided by P. Kötter, University of Frankfurt, Germany) chromosome XVI (sites YPRCΔ15 and YPRCτ3) by using a standard transformation procedure [73] and a bipartite gene targeting strategy [23]. *KanMX* as a selectable marker was looped out by methods described previously [74] and *Kluyveromyces lactis* (*K.l.*)*URA3* was looped out by selection on SD plates supplemented with 30 mg L^{-1} uracil and 750 mg L^{-1} 5-fluoroorotic acid (5-FOA), respectively. The strains harboring all MEP genes will in the following be referred to as SCISP06 and SCISP12 (Table 1).

The genes *erpA*, *fldA* and *fpr* were amplified by PCR using *E. coli* DH5α genomic DNA as a template and primers listed in Table 2. The *Not*I/*Sac*I restricted *fldA* fragment and *Bam*HI/*Xho*I restricted *fpr* fragment were cloned into pSP-GM1, a derivative of pSP-G1 [24,75]. A P$_{TDH3}$–*erpA*–T$_{PGK1}$ cassette was constructed by fusion PCR performed with Phusion high-fidelity DNA polymerase (Finnzymes, Espoo, Finland) and primer pair PGK1T-MreI-rev/ TDH3-Kpn2I-fw, restricted by *Kpn2*I/*Mre*I and cloned into pSP-GM1 containing the *fldA* and *fpr* genes. This resulted in construction of plasmid pISP08 (Figure 3B). pISP08 was transformed into strain SCISP06 resulting in formation of strain SCISP16 (Table 1).

Sequences of plant genes encoding IspG (AAN87171.1) and IspH (AAO15446.1) from *A. thaliana* were synthesized by DNA2.0 (Menlo Park, CA, USA). The sequence of *iscA* from *Homo sapiens*, *hISCA* (NP_112202.2) was synthesized by GenScript (Piscataway, NJ, USA). The sequence of *iscA* from *A. thaliana*, *CpIscA* (Q9XIK3.2) was used to construct the expression cassette, P$_{TDH3}$–*CpIscA*–T$_{PGK1}$, and this cassette was synthesized by GenScript. All synthetic genes were codon optimized for expression in *S. cerevisiae*.

The *Bam*HI/*Xho*I restricted *At-IspG* fragment and *Not*I/*Sac*I restricted *At-IspH* fragment were cloned into pSP-GM3, a derivative of the pSP-GM1 plasmid [75]. The *Pvu*II restricted fragment of pSP-GM1 including the *TEF1-PGK1* promoter region was cloned into *Pvu*II restricted pESC-HIS (Startagene,La Jolla,USA) to construct pSP-GM3. A truncated fragment of *hISCA1* encoding a protein without the mitochondrial signal peptide was amplified by PCR using the synthetic *hISCA1* as a template and primers listed in Table 2. A P$_{TDH3}$–*hISCA1*–T$_{PGK1}$ cassette was constructed by fusion PCR performed with Phusion high-fidelity DNA polymerase (Finnzymes, Espoo, Finland) and primer pair PGK1T-MreI-rev/TDH3-Kpn2I-fw. Both *Kpn2*I/ *Mre*I restricted P$_{TDH3}$–*hISCA1*–T$_{PGK1}$ and P$_{TDH3}$–*CpIscA*–T$_{PGK1}$ fragments were cloned into pSP-GM3 containing the *At-IspG* and *At-IspH* genes, respectively, resulting in pISP24 and pISP25. In the next step, pISP08 was co-transformed with either pISP24 or pISP25 (Figure 3B) into strain SCISP12 resulting in generation of strain SCISP31 and SCISP32, respectively. To create the control strain, empty plasmids, pSP-GM1 and pSP-GM3, were cloned into wild type (CEN.PK113-13D), SCISP06 and SCISP12 resulting in strains SCISP28, SCISP29 and SCISP30, respectively. The strains used in this study are listed in Table 1.

In order to delete *ERG13*, upstream and downstream flanking regions of the target gene were PCR amplified. These upstream and downstream flanking regions were fused to the 5′ and the 3′ part of the *kanMX* cassette amplified from plasmid pUG6 [74] by fusion PCR performed with Phusion high-fidelity DNA polymerase (Finnzymes). In the next step, the fused PCR fragments 1 and 2 including upstream flanking region of *ERG13*+ *loxP* - 2/3 *kanMX*

Table 2. List of oligonucleotide primers used in this study.

Primer name	Sequence
Oligonucleotide primers for verification of gene integration and transcription	
DXS up	ATGTCCTTTGATATTGCTAAATATCC
DXS down	TAGGCCAACCAAGCCTTTATC
DXR up	TGAAGCAGCTAACTATCTTGGGT
DXR down	TCGTTAAGAAGCTAGTCTCATAACTTC
ispD up	CACGACACACTTAGATGTGTGTG
ispD down	TCAAGTGTTTTCTTGGTGGATG
ispE up	ATGAGAACTCAATGGCCTTCC
ispE down	ATAACATTGCCCTATGAAGAGG
ispF up	ATGAGAATAGGTCACGGTTTCG
ispF down	TTCGTAGCCTTGATTAGCAATG
ispG up	CACAACCAAGCCCCAATACA
ispG down	TCATTTCTCCACCTGTTGGAC
ispH up	TGCAAATATTATTGGCGAATCC
ispH down	TCAATCGACCTCACGTATATCC
idi up	ATGCAGACTGAACACGTTATTCTG
idi down	TTAATTGGGTGAATGCTGACAG
URA up	GATGATGTAGTTTCTGGTTTTTAAATC
URA down	TTTAGCTTTGACATGATTAAGCTCA
KanMx up	TAGGTCTAGAGATCTGTTTAGCTTGC
KanMx down	ATTAAGGGTTCTCGAGAGCTCG
Oligonucleotide primers for gene deletions	
KanMx-1-fw	CTGAAGCTTCGTACGCTG
KanMx-1-rev	TCACCATGAGTGACGACTGA
KanMx-2-fw	TTCCAACATGGATGCTGAT
KanMx-2-rev	CTAGTGGATCTGATATCAC
ERG13-1-fw	GTTGGTGTGGTATTAAAGGA
ERG13-1-rev	<u>CAGCGTACGAAGCTTCAGGGACTTG</u>TCAATCAGAGTT
ERG13-2-fw	<u>GTGATATCAGATCCACTAGC</u>AACCTGTAAATTGGTCAC
ERG13-2-rev	CGTAAGATCTTCTAAATTTGTC
Oligonucleotide primers for verification of gene deletions	
ERG13-up-fw	TACGAGTGTGTTGAAAGTAG
ERG13-down-rev	CATTTATGAAGGGGGGTTCAG
Oligonucleotide primers for amplification of the bacterial genes	
fpr-BamHI-fw	GTTGTT**GGATCC**CAGGAGAAAAACATGGCTGA
fpr -XhoI-rev	GTTGTT**CTCGAG** CGTTTATCGATAAGTAACCGCT
fldA-Not1-fw	GTTGTT**GCGGCCGC**GAGGTTATTTCACTCATGGCT
fldA-SacI-rev	GTTGTT**GAGCTC**CATCACATCAGGCATTGAGA
ErpA -fw	ATGAGTGATGACGTAGCACT
ErpA-rev	TTAGATACTAAAGGAAGAACCGCA
PGK1T-fus-fw (erpA)	<u>TGCGGTTCTTCCTTTAGTATCTAAGG</u>TGTTGCTTTCTTATCCGA
PGK1T-MreI-rev	GTTGTT**CGCCGGCG**GGTCGCAGAATTTTCGAGTT
TDH3-Kpn2I-fw	GTTGTT**TCCGGA**CAGTTTATCATTATCAATACTCGCC
TDH3-fus-rev (erpA)	<u>AGTGCTACGTCATCACTCAT</u>GAATCCGTCGAAACTAAGTTCTGGTG
Oligonucleotide primers for amplification of the human gene	
hisca-fw	ATGGCCGCCTTGACCTTGACT
hiscA-rev	<u>TCAGATGTTGAAGGATTCACCG</u>
PGK1T-fus-fw (iscA)	<u>CGGTGAATCCTTCAACATCTGA</u>GGTGTTGCTTTCTTATCCGA
TDH3-fus-rev (iscA)	<u>AGTCAAGGTCAAGGCGGCCAT</u>GAATCCGTCGAAACTAAGTTCTGGTG

Underlined characters correspond to flanking sequences used for fusion PCR; bold characters correspond to restriction sites.
doi:10.1371/journal.pone.0052498.t002

and 2/3 *kanMX* - *loxP*+downstream flanking region of *ERG13*, respectively, were used for deletion by bipartite gene targeting [23]. Deletion of *ERG13* was verified by diagnostic PCR. For this purpose, PCR primers were designed to bind 400 to 500 bp up- and downstream of the start and stop codon, respectively (Table 2). All PCR products were sequenced.

Media Composition

The transformants were selected on minimal medium plates containing 1.7 g L^{-1} yeast nitrogen base w/o amino acids and ammonium sulfate (Formedium, Hunstanton, England), 5 g L^{-1} ammonium sulfate, 0.77 g L^{-1} complete supplement mixture (CSM w/o uracil or CSM w/o uracil and histidine) (MP Biomedicals, Solon, OH, USA), 20 g L^{-1} glucose and 20 g L^{-1} agar. In media containing G418, 0.86 g L^{-1} L-glutamic acid monosodium salt monohydrate was used instead of ammonium sulfate. Filter sterilized G418 disulfide salt (Sigma-Aldrich, St. Louis, MO) was added to the media before plating to a final concentration of 200 mg L^{-1}. Mevalonic acid lactone (Sigma-Aldrich) was prepared as a 500 mg L^{-1} stock solution in 2 N NaOH, incubated at 37°C for 30 min, filter sterilized, and then added to the media to reach a final concentration of 10 mg L^{-1}. For anaerobic cultivations 125 μL ergosterol was added to the media from a stock solution (1 g L^{-1}) that was prepared as described previously [76]. Lovastatin (Sigma) was hydrolyzed in ethanolic sodium hydroxide (15% (v/v) ethanol, 0.25% (w/v) NaOH) at 60°C for 1 h. After cooling down to room temperature, it was added to shake flasks at a final concentration of 2 g L^{-1}.

Batch Cultivation

Cotton-stopped, 50 mL Erlenmeyer flasks were used for evaluation of the MEP pathway functionality using lovastatin. The shake flasks contained 10 mL medium with the above mentioned composition. 50 mL falcon tubes containing 5 mL medium were used for seed cultures. Both seed tubes and shake flasks were incubated at 30°C and agitated in an orbital shaker at 180 rpm. Pre-cultures were used to inoculate the shake flasks to a final dry weight of 1 mg L^{-1}. Cell growth was monitored by measuring the optical density at 600 nm using a Genesis20 spectrophotometer (Thermo Scientific, Madison, WI, USA). All cultivations were performed in triplicate.

Supporting Information

File S1 File represents DNA sequences of the four synthetic fragments which are carrying eight codon optimized bacterial genes for expression in *S. cerevisiae*. For more information see text.
(PDF)

References

1. Nour-Eldin HH, Hansen BG, Nørholm MHH, Jensen JK, Halkier BA (2006) Advancing uracil-excision based cloning towards an ideal technique for cloning PCR fragments. Nucleic Acids Res 34: e122.
2. Geu-Flores F, Nour-Eldin HH, Nielsen MT, Halkier BA (2007) USER fusion: a rapid and efficient method for simultaneous fusion and cloning of multiple PCR products. Nucleic Acids Res 35: e55.
3. Shao Z, Zhao H, Zhao H (2009) DNA assembler, an in vivo genetic method for rapid construction of biochemical pathways. Nucleic Acids Res 37: e16.
4. Martin VJJ, Pitera DJ, Withers ST, Newman JD, Keasling JD (2003) Engineering a mevalonate pathway in *Escherichia coli* for production of terpenoids. Nature Biotechnol. 21: 796–802.
5. Szczebara FM, Chandelier C, Villeret C, Masurel A, Bourot S, et al. (2003) Total biosynthesis of hydrocortisone from a simple carbon source in yeast. Nature Biotechnol 21: 143–149.
6. Yan Y, Kohli A, Koffas MAG (2005) Biosynthesis of natural flavanones in *Saccharomyces cerevisiae*. Appl Environ Microbiol 71: 5610–5613.
7. Maury J, Asadollahi MA, Møller K, Clark A, Nielsen J (2005) Microbial isoprenoid production: An example of green chemistry through metabolic engineering. Adv Biochem Eng Biotechnol 100: 19–51.
8. Rohmer M, Knani M, Simonin P, Sutter B, Sahm H (1993) Isoprenoid biosynthesis in bacteria: a novel pathway for the early steps leading to isopentenyl diphosphate. Biochemical J 295: 517–524.
9. Arigoni D, Sagner S, Latzel C, Eisenreich W, Bacher A, et al. (1997) Terpenoid biosynthesis from 1-deoxy-D-xylose in higher plants by intramolecular skeletal rearrangement. Proc Natl Acad Sci USA 94: 10600–10605.
10. Sprenger GA, Schörken U, Wiegert T, Grolle S, de Graaf AA, et al. (1997) Identification of a thiamin-dependent synthase in *Escherichia coli* required for the formation of the 1-deoxy-D-xylulose 5-phosphate precursor to isoprenoids, thiamin, and pyridoxol. Proc Natl Acad Sci USA 94: 12857–12862.
11. Takahashi S, Kuzuyama T, Watanabe H, Seto HA (1998) 1-deoxy-D-xylulose 5-phosphate reductoisomerase catalyzing the formation of 2-C-methyl-D-erythritol 4-phosphate in an alternative nonmevalonate pathway for terpenoid biosynthesis. Proc Natl Acad Sci USA 95: 9879–9884.
12. Rohdich F, Wungsintaweekul J, Fellermeier M, Sagner S, Herz S, et al. (1999) isoprenoids: YgbP protein of *Escherichia coli* catalyzes the formation of 4-diphosphocytidyl-2-C-methylerythritol. Proc Natl Acad Sci USA 96: 11758–11763.
13. Lüttgen H, Rohdich F, Herz S, Wungsintaweekul J, Hecht S, et al. (2000) Biosynthesis of terpenoids: YchB protein of *Escherichia coli* phosphorylates the 2-hydroxy group of 4-diphosphocytidyl-2C-methyl-D-erythritol. Proc Natl Acad Sci USA 97: 1062–1067.
14. Herz S, Wungsintaweekul J, Schuhr CA, Hecht S, Luttgen H, et al. (2000) Biosynthesis of terpenoids: YgbB protein converts 4-diphosphocytidyl-2C-methyl-D-erythritol 2-phosphate to 2C-methyl-D-erythritol 2,4-cyclodiphosphate. Proc Natl Acad Sci USA 97: 2486–2490.
15. Adam P, Hecht S, Eisenreich W, Kaiser J, Grawert T, et al. (2002) Biosynthesis of terpenes: studies on 1-hydroxy-2-methyl-2-(E)-butenyl 4-diphosphate reductase. Proc Natl Acad Sci USA 99: 12108–12113.
16. Querol J, Campos N, Imperial S, Boronat A, Rodríguez-Concepción M (2002) Functional analysis of the *Arabidopsis thaliana* GCPE protein involved in plastid isoprenoid biosynthesis. FEBS Lett 514: 343–346.
17. Rohdich F, Zepeck F, Adam P, Hecht S, Kaiser J, et al. (2003) The deoxyxylulose phosphate pathway of isoprenoid biosynthesis: studies on the mechanisms of the reactions catalyzed by IspG and IspH protein. Proc Natl Acad Sci USA 100: 1586–91.
18. Wolff M (2003) Isoprenoid biosynthesis via the methylerythritol phosphate pathway: the (E)-4-hydroxy-3-methylbut-2-enyl diphosphate reductase (LytB/IspH) from *Escherichia coli* is a [4Fe–4S] protein. FEBS Lett 541: 115–120.
19. Ro DK, Paradise EM, Ouellet M, Fisher KJ, Newman KL, et al. (2006) Production of the antimalarial drug precursor artemisinic acid in engineered yeast. Nature 440: 940–943.
20. Dejong JM, Liu Y, Bollon AP, Long RM, Jennewein S, et al. (2006) Genetic engineering of taxol biosynthetic genes in *Saccharomyces cerevisiae*. Biotechnol Bioeng 93: 212–224.
21. Maury J, Asadollahi MA, Møller K, Schalk M, Clark A, et al. (2008) Reconstruction of a bacterial isoprenoid biosynthetic pathway in *Saccharomyces cerevisiae*. FEBS Lett 582: 4032–4038.
22. Nookaew I, Jewett MC, Meechai A, Thammarongtha C, Laoteng K, et al. (2008) The genome-scale metabolic model iIN800 of *Saccharomyces cerevisiae* and its validation: a scaffold to query lipid metabolism. BMC Sys Biol 2: 71.
23. Erdeniz N, Mortensen UH, Rothstein R (1997) Cloning-free PCR-based allele replacement methods. Genome Res 1174–1183.
24. Partow S, Siewers V, Bjørn S, Nielsen J, Maury J (2010) Characterization of different promoters for designing a new expression vector in *Saccharomyces cerevisiae*. Yeast 27: 955–964.
25. Flagfeldt DB, Siewers V, Huang L, Nielsen J (2009) Characterization of chromosomal integration sites for heterologous gene expression in *Saccharomyces cerevisiae*. Yeast 26: 545–551.
26. Servouse M, Mons N, Baillargeat JL, Karst F (1984) Isolation and characterization of yeast mutants blocked in mevalonic acid formation. Biochem Biophys Res Commun 123: 424–430.

27. Alberts AW, Chen J, Kuron G, Hunt V, Huff J, et al. (1980) Mevinolin: a highly potent competitive inhibitor of hydroxymethylglutaryl-coenzyme A reductase and a cholesterol-lowering agent. Proc Natl Acad Sci USA 77: 3957–61.

28. Formenti LR (2011) Isoprenoid production in yeast through the bacterial MEP pathway. PhD thesis. *Center for Microbial Biotechnology, DTU, Denmark.*

29. Seemann M, Wegner P, Schünemann V, Bui BTS, Wolff M, et al. (2005) Isoprenoid biosynthesis in chloroplasts via the methylerythritol phosphate pathway: the (E)-4-hydroxy-3-methylbut-2-enyl diphosphate synthase (GcpE) from *Arabidopsis thaliana* is a [4Fe-4S] protein. J Biol Inorg Chem 10: 131–137.

30. Altincicek B, Duin EC, Reichenberg A, Hedderich R, Kollas AK, et al. (2002) LytB protein catalyzes the terminal step of the 2-C-methyl-D-erythritol-4-phosphate pathway of isoprenoid biosynthesis. FEBS Lett 532: 437–440.

31. Gräwert T, Span I, Eisenreich W, Rohdich F, Eppinger J, et al. (2010) Probing the reaction mechanism of IspH protein by x-ray structure analysis. Proc Natl Acad Sci USA 107: 1077–1081.

32. Gräwert T, Kaiser J, Zepeck F, Laupitz R, Hecht S, et al. (2004) IspH protein of *Escherichia coli*: studies on iron-sulfur cluster implementation and catalysis. J Am Chem Soc 126: 12847–12855.

33. Loiseau L, Gerez C, Bekker M, Ollagnier-de Choudens S, Py B, et al. (2007) ErpA, an iron sulfur (Fe S) protein of the A-type essential for respiratory metabolism in *Escherichia coli*. Proc Natl Acad Sci USA 104: 13626–13631.

34. Puan KJ, Wang H, Dairi T, Kuzuyama T, Morita CT (2005) fldA is an essential gene required in the 2-C-methyl-D-erythritol 4-phosphate pathway for isoprenoid biosynthesis. FEBS Lett 579: 3802–3806.

35. Jenkins CM, Waterman MR (1994) Flavodoxin and NADPH-flavodoxin reductase from *Escherichia coli* support bovine cytochrome P450c17 hydroxylase activities. J Biol Chem 269: 27401–27408.

36. Dimster-Denk D, Rine J (1996) Transcriptional regulation of a sterol-biosynthetic enzyme by sterol levels in *Saccharomyces cerevisiae*. Mol Cell Biol 16: 3981–3989.

37. Vinella D, Brochier-Armanet C, Loiseau L, Talla E, Barras F (2009) Iron-sulfur (Fe/S) protein biogenesis: phylogenomic and genetic studies of A-type carriers. PLoS Genet 5: e1000497.

38. Song D, Tu Z, Lee FS (2009) Human ISCA1 interacts with IOP1/NARFL and functions in both cytosolic and mitochondrial iron-sulfur protein biogenesis. J Biol Chem 284: 35297–307.

39. Abdel-Ghany SE, Ye H, Garifullina GF, Zhang L, Pilon-Smits EAH, Pilon M (2005) Iron-sulfur cluster biogenesis in chloroplasts. Involvement of the scaffold protein CpIscA. Plant Physiol 138: 161–172.

40. Liochev S, Fridovich I (1994) The role of O₂‾ in the production of HO: in vitro and in vivo. Free Rad Biol Med 16: 29–33.

41. Pantopoulos K, Hentze MW (1995) Rapid responses to oxidative stress mediated by iron regulatory protein. EMBO J 14: 2917–24.

42. Förster J, Famili I, Fu P, Palsson BØ, Nielsen J (2003) Genome-scale reconstruction of the *Saccharomyces cerevisiae* metabolic network. Genome Res 13: 244–253.

43. Asadollahi MA, Maury J, Patil KR, Schalk M, Clark A, Nielsen J (2009) Enhancing sesquiterpene production in *Saccharomyces cerevisiae* through in silico driven metabolic engineering. Metab Eng 11: 328–334.

44. Piddocke MP, Fazio A, Vongsangnak W, Wong ML, Heldt-Hansen HP, et al. (2011) Revealing the beneficial effect of protease supplementation to high gravity beer fermentations using "-omics" techniques. Microb Cell Factories 10: 27.

45. Ajikumar PK, Xiao WH, Tyo KE, Wang Y, Simeon F, et al. (2010) Isoprenoid pathway optimization for Taxol precursor overproduction in *Escherichia coli*. Science 330: 70–4.

46. Dugar D, Stephanopoulos G (2011) Relative potential of biosynthetic pathways for biofuels and bio-based products. Nat biotechnol 29: 1074–8.

47. Wingler LM, Cornish VW (2011) Reiterative Recombination for the in vivo assembly of libraries of multigene pathways. Proc Natl Acad Sci USA 108(37): 15135–15140.

48. Kosuri S, Eroshenko N, LeProustet EM, Super M, Way J, et al. (2010) Scalable gene synthesis by selective amplification of DNA pools from high-fidelity microchips. Nat biotechnol 28: 1295–9.

49. Matzas M, Stahler PF, Kefer N, Siebelt N, Boisguerin V, et al. (2010) High-fidelity gene synthesis by retrieval of sequence-verified DNA identified using high-throughput pyrosequencing. Nat biotechnol 28: 1291–4.

50. Gustafsson C, Govindarajan S, Minshull J (2004) Codon bias and heterologous protein expression. Trends in biotechnology 22: 346–53.

51. Ikemura T (1981) Correlation between the abundance of *Escherichia coli* transfer RNAs and the occurrence of the respective codons in its protein genes: a proposal for a synonymous codon choice that is optimal for the *E. coli* translational system. J Mol Biol 151: 389–409.

52. Lorenz RT, Parks LEOW, Carolina N (1990) Effects of lovastatin (mevinolin) on sterollevels and of azoles in *Saccharomyces cerevisiae*. Microbiology 34: 1660–1665.

53. Bergès T, Guyonnet D, Karst F (1997) The *Saccharomyces cerevisiae* mevalonate diphosphate decarboxylase is essential for viability and a single Leu-to-Pro mutation in a conserved sequence leads to thermosensitivity. J Bacteriol 179: 4664–4670.

54. Jennings SM, Tsay YH, Fisch TM, Robinson GW (1991) Molecular cloning and characterization of the yeast gene for squalene synthetase. Proc Natl Acad Sci USA 88: 6038–42.

55. Tsay YH, Robinson GW (1991) Cloning and characterization of ERG8, an essential gene of *Saccharomyces cerevisiae* that encodes phosphomevalonate kinase. Mol Cell Biol 11: 620–31.

56. Kuranda K, François J, Palamarczyk G (2010) The isoprenoid pathway and transcriptional response to its inhibitors in the yeast *Saccharomyces cerevisiae*. FEMS Yeast Res 10: 14–27.

57. Kuranda K, Grabinska K, Berges T, Karst F, Leberre V, et al. (2009) The *YTA7* gene is involved in the regulation of the isoprenoid pathway in the yeast *Saccharomyces cerevisiae*. FEMS Yeast Res 9: 381–90.

58. Boguta M, Czerska K, Zoładek T (1997) Mutation in a new gene *MAF1* affects tRNA suppressor efficiency in *Saccharomyces cerevisiae*. Gene 185: 291–6.

59. Kamińska J, Grabinska K, Kwapisz M, Sikora J, Smagowicz WJ, et al. (2002) The isoprenoid biosynthetic pathway in *Saccharomyces cerevisiae* is affected in a *maf1–1* mutant with altered tRNA synthesis. FEMS Yeast Res 2: 31–7.

60. Dihanich ME, Najarian D, Clark R, Gillman EC, Martin NC, et al. (1987) Isolation and characterization of *MOD5*, a gene required for isopentenylation of cytoplasmic and mitochondrial tRNAs of *Saccharomyces cerevisiae*. Mol Cell Bio 7: 177–184.

61. Seemann M, Tse Sum Bui B, Wolff M, Miginiac-Maslow M, Rohmer M (2006) Isoprenoid biosynthesis in plant chloroplasts via the MEP pathway: direct thylakoid/ferredoxin-dependent photoreduction of GcpE/IspG. FEBS Lett 580: 1547–1552.

62. Xiao Y, Zhao ZK, Liu P (2008) Mechanistic studies of IspH in the deoxyxylulose phosphate pathway: heterolytic C-O bond cleavage at C4 position. J Am Chem Soc 130: 2164–2165.

63. Xiao Y, Chu L, Sanakis Y, Liu P (2009) Revisiting the IspH catalytic system in the deoxyxylulose phosphate pathway: achieving high activity. J Am Chem Soc 131: 9931–9933.

64. Mühlenhoff U, Richhardt N, Gerber J, Lill R (2002) Characterization of iron-sulfur protein assembly in isolated mitochondria. A requirement for ATP, NADH and reduced iron. J Biol Chem 277: 29810–29816.

65. Sharma AK, Pallesen LJ, Spang RJ, Walden WE (2010) Cytosolic iron-sulfur cluster assembly (CIA) system: factors, mechanism, and relevance to cellular iron regulation. J Biol Chem 285: 26745–26751.

66. Lill R, Mühlenhoff U (2005) Iron-sulfur-protein biogenesis in eukaryotes. Trends Biochem Sci 30: 133–141.

67. Pinske C, Sawers RG (2012) A-type carrier protein ErpA is essential for formation of an active formate-nitrate respiratory pathway in *Escherichia coli* K-12. J Bacteriology 194: 346–53.

68. Gerber J, Neumann K, Prohl C, Mu U, Lill R (2004) The yeast scaffold proteins Isu1p and Isu2p are required inside mitochondria for maturation of cytosolic Fe/S Proteins. Mol Cell Biol 24: 4848–4857.

69. Tan G, Lu J, Bitoun JP, Huang H, Ding H (2009) IscA/SufA paralogues are required for the [4Fe-4S] cluster assembly in enzymes of multiple physiological pathways in *Escherichia coli* under aerobic growth conditions. Biochem J 420: 463–72.

70. Culotta VC (2000) Iron Homeostasis. Mol Cell Biol 20: 3918–3927.

71. Kaut A, Lange H, Diekert K, Kispal G, Lill R (2000) Isa1p is a component of the mitochondrial machinery for maturation of cellular iron-sulfur proteins and requires conserved cysteine residues for function. J Biol Chem 275: 15955–61.

72. Muhlenhoff U, Richter N, Pines O, Pierik AJ, Lill R (2011) Specialized function of yeast Isa1 and Isa2 in the maturation of mitochondrial [4Fe-4S] proteins. J Biol Chem 1–22.

73. Gietz RD, Woods RA (2002) Transformation of yeast by lithium acetate/single-stranded carrier DNA/polyethylene glycol method. Methods Microbiol 350: 87–96.

74. Güldener U, Heck S, Fielder T, Beinhauer J, Hegemann JH (1996) A new efficient gene disruption cassette for repeated use in budding yeast. Nucleic Acids Res 24: 2519–24.

75. Chen Y, Partow S, Scalcinati G, Siewers V, Nielsen J (2012) Enhancing the copy number of episomal plasmids in *Saccharomyces cerevisiae* for improved protein production. FEMS Yeast Res 1–10.

76. Verduyn C, Postma E, Scheffers WA, van Dijken JP (1992) Effect 432 of benzoic acid on metabolic fluxes in yeasts: A continous-culture study on regulation of respiration and alcoholic fermentation. Yeast 8: 501–517.